Chapter 5
Modelling Phosphorus Dynamics in the Soil–Plant System

Andrea Schnepf, Daniel Leitner, Sabine Klepsch, Sylvain Pellerin, and Alain Mollier

5.1 Introduction

The importance of phosphorus (P) as both sparingly mobile essential nutrient and pollutant is reflected by the large number of P models at different scales and with different purposes. P dynamics have been studied at a wide range of spatial scales. Examples include the global scale (Harrison et al. 2005), watershed scale (Radcliffe et al. 2009), ecosystem scale (Schlecht and Hiernaux 2005), farming systems scale (Schils et al. 2007), field scale (Schoumans and Groenendijk 2000; Torbert et al. 2008), whole plant scale (Mollier et al. 2008), soil profile scale (Roose and Fowler 2004), and single root scale (Kirk 1999; Roose et al. 2001). The positions of the various P models in a space–time diagram (Fig. 5.1) illustrate the main temporal and spatial scales of application. Most of the models are mechanistic and deterministic; the degree of empiricalness generally increases with spatial scale.

The applications for which P models have been used include carbon uptake by the terrestrial biosphere (Wang et al. 2007), effect of tectonic uplift and erosion on P availability in soil (Porder et al. 2007), water quality due to agricultural

---

A. Schnepf (✉) and D. Leitner
Department of Forest and Soil Sciences, Institute of Soil Science, BOKU – University of Natural Resources and Life Sciences Vienna, Peter Jordan Strasse 82, 1190 Vienna, Austria
e-mail: andrea.schnepf@boku.ac.at; daniel.leitner@boku.ac.at

S. Klepsch
Department of Forest and Soil Sciences, Institute of Soil Science, BOKU – University of Natural Resources and Life Sciences Vienna, Peter Jordan Strasse 82, 1190 Vienna, Austria
and
Health & Environment Department, Environmental Resources & Technologies, AIT Austrian Institute of Technology, 2444 Seibersdorf, Austria
e-mail: sabine.klepsch@boku.ac.at

S. Pellerin and A. Mollier
Department for the Environment and Agronomy, Joint Research Unit for Soil–Plant Transfer and the Cycle of Nutrients and Trace Elements (TCEM), National Institute for Agricultural Research (INRA), 71, Avenue Edouard Bourlaux, BP 81, 33883 Villenave d'Ornon Cedex, France
e-mail: pellerin@bordeaux.inra.fr; mollier@bordeaux.inra.fr

E.K. Bünemann et al. (eds.), *Phosphorus in Action*, Soil Biology 26,
DOI 10.1007/978-3-642-15271-9_5,

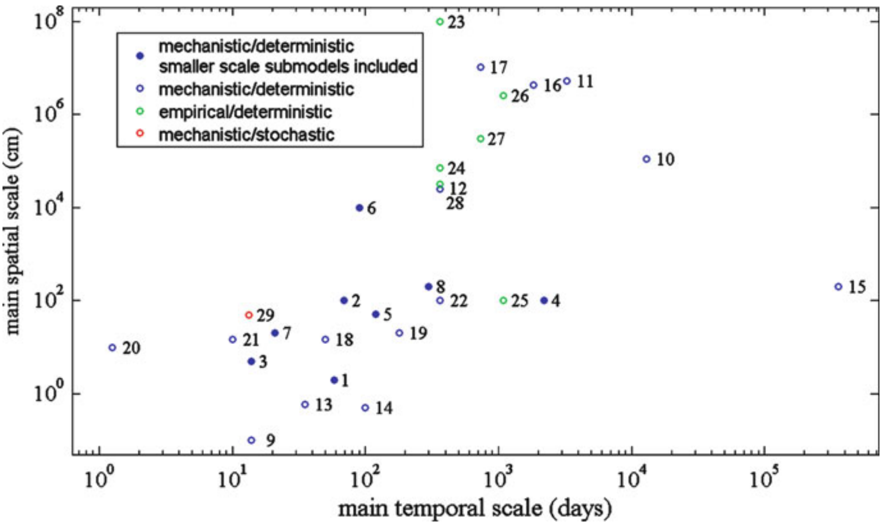

Fig. 5.1 Space–time diagram of commonly used P models. *Closed symbols* indicate that this specific model includes smaller-scale submodels. The *colour* illustrates whether the model is mechanistic or empirical, deterministic or stochastic. References for model numbers: *1* Ptashnyk et al. (2010), *2* Shi and Erickson (2001), *3* Schnepf and Roose (2006), *4* Grant et al. (2004), *5* Roose and Fowler (2004), *6* Mollier et al. (2008), *7* Bhadoria et al. (2002), *8* Dunbabin et al. (2009), *9* Hofflmann et al. (1994), *10* Torbert et al. (2008), *11* Radcliffe et al. (2009), *12* Schoumans and Groenendijk (2000), *13* Kirk (1999), *14* Roose et al. (2001), *15* Porder et al. (2007), *16* Arheimer et al (2004), *17* Migliaccio et al. (2007), *18* Huguenin-Elie et al. (2009), *19* Reginato et al. (2000), *20* Overman and Scholtz (1999), *21* Grant and Robertson (1997), *22* Landis and Fraser (2008), *23* Harrison et al. (2005), *24* Schils et al. (2007), *25* Chung et al. (2003), *26* Dalzell et al. (2004), *27* Djodjic et al. (2002), *28* Giasson et al. (2002), *29* Ge et al. (2000)

management practices (Arheimer et al. 2004; Chung et al. 2003; Dalzell et al. 2004; Djodjic et al. 2002; Grant et al. 2004; Migliaccio et al. 2007), P uptake from soil by root systems (Leitner et al. 2010a; Roose and Fowler 2004), root P uptake and P efficiency (Bhadoria et al. 2002; Huguenin-Elie et al. 2009; Kirk 1999; Reginato et al. 2000), crop response to soil P levels (Mollier et al. 2008), competing root systems (Smethurst and Comerford 1993), manure management and fertiliser optimisation (Dunbabin et al. 2009; Giasson et al. 2002; Teklić et al. 2002), P as amendment in in-situ stabilisation of lead (Pb)-contaminated soils (Shi and Erickson 2001), P sorption in soil (Overman and Scholtz 1999; Van Der Zee and Van Riemsdijk 1991), P uptake by root hairs and mycorrhizal fungi (Grant and Robertson 1997; Landis and Fraser 2008; Leitner et al. 2010b; Schnepf and Roose 2006; Schnepf et al. 2008b), biodiversity (Fitter et al. 2005) and forest growth response (Gillespie and Pope 1990; Kirschbaum et al. 1998). Reviews describing models for plant solute uptake are given by Tinker and Nye (2000), Darrah et al. (2006) and Luster et al. (2009).

Many of these models are based on generic software, and it is often not apparent what the underlying equations and assumptions are. This could lead to inappropriate applications and erroneous model outputs. Moreover, the applicability of such models is limited to the specific purpose for which each was designed, making it problematic to extend a particular model for a slightly different aim. This calls for documenting the underlying theory and mathematical basis of any model in a form that can be understood by non-experts. Furthermore, nowadays a set of mathematical equations can be solved relatively easily by flexible software packages (e.g. Comsol Multiphysics, FlexPDE).

5.1.1 Building a Mathematical Model

A mathematical model is a simplified description of reality in terms of mathematical equations. For many scientific problems, models can help to quantify expected results, compare the effects of alternative theories, describe the effect of complex factors, explain how underlying processes contribute to the observed results, extrapolate results to other situations, or predict future events (Smith and Smith 2007). In order to make the model most meaningful and least prone to errors, it should be as simple as possible, but not any simpler. In the words of Einstein (1934): “It can scarcely be denied that the supreme goal of all theory is to make the irreducible basic elements as simple and as few as possible without having to surrender the adequate representation of a single datum of experience.”

Each model is built for a specific purpose and starts from prior knowledge and hypotheses about the system. This will influence the type of model chosen and the corresponding mathematical equations used to describe the system. Models are generally classified as deterministic or stochastic and as mechanistic or empirical. Each model needs data for parameterisation; if some of the data are incompletely known; model calibration is required to determine these values accurately from available measurements (Janssen and Heuberger 1995).

Finally, accuracy, sensitivity and uncertainty analyses should be made for quantitative model evaluation (Saltelli et al. 2000; Smith and Smith 2007). Model development can be an iterative process if the model is found to be inappropriate after evaluation. In this chapter, we focus on building mathematical models based on the objectives and prior knowledge.

5.1.2 Aims of This Chapter

We illustrate model building for understanding P dynamics in the plant–soil system using three case studies. The studies focus on the traits that enhance plant P uptake from soil: mycorrhizal associations and root architecture, as well as on crop responses to soil P levels.

5.2 Modelling Case Studies

5.2.1 P Uptake by Mycorrhizal Roots

5.2.1.1 Aim of the Model

The soil volume that a plant root can exploit for sparingly soluble nutrients such as P increases enormously due to mycorrhizal roots. Non-mycorrhizal parts of a root typically have a depletion zone that is less than 5 mm wide, whereas the depletion zone of mycorrhizal root parts can reach several centimetres into the soil. Thus, mycorrhizal fungi can increase soil P availability to plants. It may be possible to exploit symbioses between various crop plants and mycorrhizal fungi to reduce the use of mineral fertilisers in agricultural management (Frossard et al. 2000). The model presented here helps to estimate how much P fertiliser could be substituted in this way, a topic especially important because of the anticipated insufficient future mineral phosphate supply (Lambers et al. 2006). This examplary simulation study is designed to quantify the effect of arbuscular mycorrhizal fungi on plant P nutrition.

In this case study, we demonstrate how to quantify soil phosphate (P_i) depletion and P_i influx into a plant root colonised by arbuscular mycorrhizal fungi using the model of Schnepf and Roose (2006) and Schnepf et al. (2008a, b). Three arbuscular mycorrhizal fungi with different growth strategies are considered. The first growth strategy describes a fungus with tip splitting proportional to the hyphal tip density (linear branching); the second assumes that branching ceases at a given maximal hyphal tip density (nonlinear branching); and the third describes a fungus that develops a highly interconnected mycelium (anastomosis).

We consider a single root with different fungal mycelia that correspond to the three growth strategies. As described in Schnepf and Roose (2006) and Schnepf et al. (2008b), P_i transport in soil is described by the diffusion equation. Furthermore, we assume that P_i is taken up by root and hyphae according to Michaelis–Menten kinetics. Previous simulations were performed in one-dimensional Cartesian coordinates in order to be consistent with validation experiments performed in compartment systems (e.g. as used by Li et al. 1991). The present study focuses on a single mycorrhizal root and therefore uses cylindrical coordinates.

5.2.1.2 Model Description

The chosen modelling approach is based on coupling a fungal growth and P_i uptake model with a classical single root model. The classical single root model (Barber 1995; Tinker and Nye 2000) is extended by a sink term for P_i uptake from soil due to arbuscular mycorrhizal hyphae [see (5.1)]. The model is given by the following equations:

$$(\theta + b)\frac{\partial c}{\partial t} = \frac{1}{r}\frac{\partial}{\partial r}\left(D\theta f r \frac{\partial c}{\partial r}\right) - 2r_{\mathrm{h}}\pi\rho(r,t)\frac{F_m c}{K_m + c}\,, \tag{5.1}$$

$$c = c_0 \quad \text{at} \quad t = 0\,, \tag{5.2}$$

$$D\theta f \frac{\partial c}{\partial r} = \frac{F_m c}{K_m + c}, \quad \text{at} \quad r = r_0\,, \tag{5.3}$$

$$D\theta f \frac{\partial c}{\partial r} = 0, \quad \text{at} \quad r = r_1, \tag{5.4}$$

where c is concentration of phosphate in soil solution, t time, r radial distance from root axis, θ volumetric water content, b buffer power, f impedance factor, D diffusion coefficient in water, c_0 initial $\mathrm{P_i}$ concentration in soil solution, r_h hyphal radius, r_0 root radius, r_1 mean half distance between roots, F_m maximal $\mathrm{P_i}$ influx into root, K_m Michaelis–Menten constant and ρ hyphal length density.

The hyphal length density, ρ, is determined using a continuous and spatially explicit hyphal population growth model (Schnepf et al. 2008a). It calculates hyphal tip and length densities based on elongation of the region just behind the hyphal tip, branching due to tip splitting, anastomosis, and tip and hyphal death. Calibration of this model to experimental data (Jakobsen et al. 1992) indicated that all three presented growth strategies occurred. The parameters found in that calibration study (Schnepf et al. 2008a) are used in the following simulations. Model equations for the hyphal tip density n and the hyphal length density ρ are given by:

$$\frac{\partial n}{\partial t} = -\frac{1}{r}\frac{\partial}{\partial r}(rnv) + F, \tag{5.5}$$

$$\frac{\partial \rho}{\partial t} = nv - d\rho\,, \tag{5.6}$$

$$F = \underbrace{b_n n\left(1 - \frac{n}{n_{\max}}\right)}_{branching} - \underbrace{a_1 n^2 - a_2 n\rho}_{anastomosis} - \underbrace{d_n n}_{tipdeath}\,, \tag{5.7}$$

$$n = 0, \rho = 0 \quad \text{at} \quad t = 0, \tag{5.8}$$

$$n = f_{\mathrm{b}}(t) \quad \text{at} \quad r = r_0\,, \tag{5.9}$$

where n is hyphal tip density, ρ hyphal length density, v tip elongation rate, d hyphal death rate, b_n branching rate, $n_{\max}$ maximal tip density, a_1 and a_2 tip-tip and tip-side anastomosis rates, d_n tip death rate, f_{b} tip density at the root interface and F is the rate of creation or destruction of hyphal tips.

Equations (5.5)–(5.9) were solved with a Lax–Wendroff-scheme (Morton and Mayers 1994). Equations (5.1)–(5.4) were solved with the finite element method using Comsol multiphysics.

5.2.1.3 Results

Figure 5.2 shows a two-dimensional visualisation of the colony shapes resulting from the different fungal growth strategies. Simulations are based on a discrete L-system model, which approximates the continuous model given by (5.5)–(5.9). The hyphal length densities and P_i depletion at different distances from the root after 21 days are shown in Fig. 5.3. The different fungal growth strategies clearly yield different patterns of extraradical hyphal length densities and thus different P_i depletion radii of the mycorrhizal roots. The radius of the zone where more than half of the initial P_i concentration has been depleted is 1.5 cm for the linear branching strategy, 3 cm for nonlinear branching and 6 cm for anastomosis.

Figure 5.4 shows the resulting influx of P_i into root and hyphae. In all cases, influx into fungus exceeds that into root by an order of magnitude. Influx into root decreases quickly with time, whereas influx into fungus increases as the colony grows. For the two nonlinear growth strategies, this can decrease with time because the fungal colony covers a large area that is already depleted and, thus, additional P_i is taken up only at the front of the colony. This is shown more explicitly in Fig. 5.4, where P_i influx into hyphae per unit hyphal length, i.e. colony efficiency, is plotted against time.

5.2.1.4 Discussion and Outlook

The results show that, as soon as the fungal colony is sufficiently large, mycorrhizal P_i influx is up to an order of magnitude larger than root P_i influx. This is particularly pronounced in the linear branching case, where the fungal hyphae compete for P_i inside the root depletion zone. The anastomosis case, in contrast, makes more use of the soil volume near the front of the fungal colony, outside the root P_i depletion zone, so that the root contribution is higher. However, fungal P_i uptake dominates overall P_i uptake in all cases, supporting the idea that roots can completely rely on the fungus for their P_i nutrition (Smith et al. 2003). The hyphal length density in the

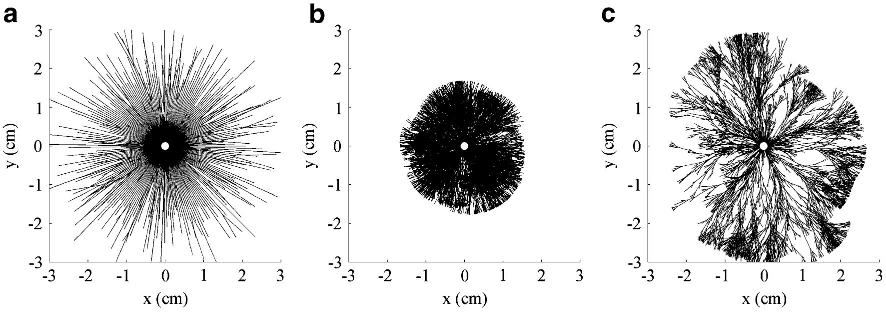

Fig. 5.2 Visualisation of (**a**) linear branching, (**b**) nonlinear branching and (**c**) anastomosis growth strategies of arbuscular mycorrhizal fungi after 14 days

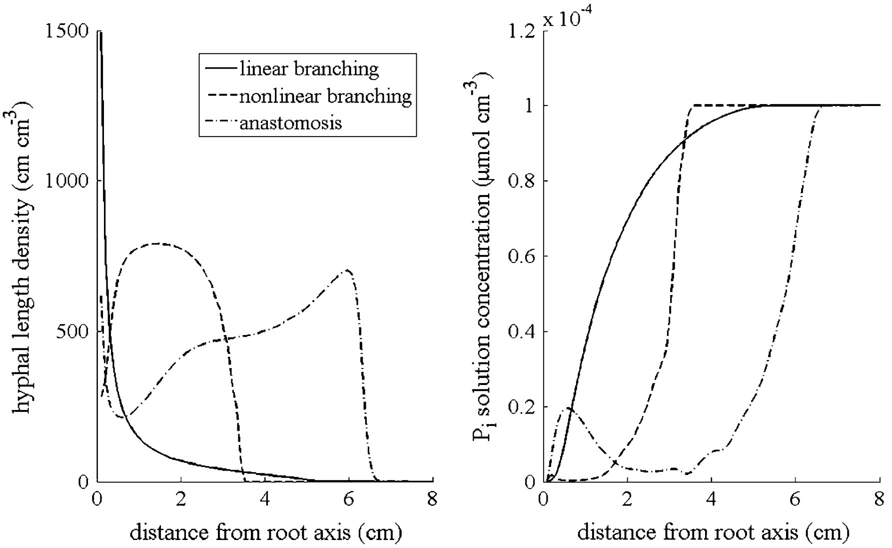

Fig. 5.3 Hyphal length densities (*left*) and P_i solution concentration around the root (*right*) corresponding to the linear branching, nonlinear branching and anastomosis growth strategies of arbuscular mycorrhizal fungi, assuming that root and fungi have the same P_i uptake parameters

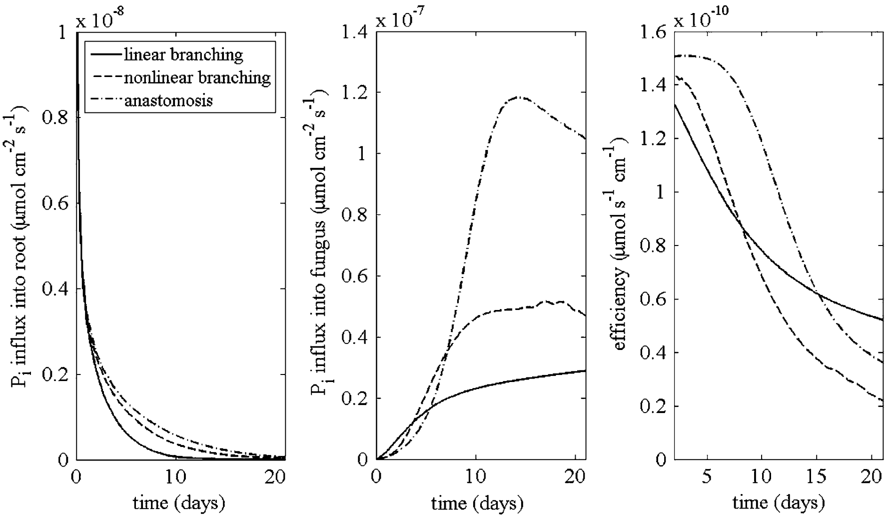

Fig. 5.4 P_i influx per unit root surface area due to root (*left*) and hyphae (*centre*) corresponding to the linear branching, nonlinear branching and anastomosis growth strategies of arbuscular mycorrhizal fungi. P_i influx per unit hyphal length (*right*)

linear branching case is high near the root surface but low further away. Accordingly, it is initially less efficient than the two other growth strategies. The nonlinear branching and anastomosis strategies result in a higher P_i influx into hyphae, but they are less efficient when relating this influx to the colony size produced.

The predicted hyphal length densities and P_i concentrations in Schnepf et al. (2008b) were based on simulations in one-dimensional Cartesian coordinates. This geometry is appropriate for a validation experiment using a compartment system in which a membrane separates a root from a purely hyphal compartment (e.g. as used by Li et al. 1991). In the present case study, we used cylindrical geometry appropriate for an individual root. This changes the shape of predicted hyphal length density and P_i depletion because, in cylindrical geometry, the same number of hyphae grow into a soil volume (which increases with distance from the root surface). Compared to Cartesian geometry, the linear branching strategy has a lower hyphal length density further away from the root surface. For the nonlinear branching strategy, the maximal tip density is reached faster near the root surface than further away and, similarly, anastomosis occurs more likely near the root surface than further away. This reduces hyphal length density near the root surface compared to Cartesian geometry.

Schnepf et al. (2008b) simulated differences with regard to P_i uptake sites along the individual hyphae. Compared with published values of P influx into mycorrhizal plants and soil P depletion, their results suggest that P_i uptake occurs not only at the tip but also at parts of the mycelium that are metabolically active. Nonetheless, a spatially explicit model for the spread of mycorrhizal mycelium and active parts is still missing. Assuming Michaelis–Menten kinetics for uptake might also oversimplify the actual uptake process. The molecular and biochemical characterisation of the corresponding P_i transport systems is currently being extensively studied (Bucher 2007; Raghothama and Karthikeyan 2005). Thus, more experimental data for parameterisation and validation are required.

5.2.2 P Uptake by a Root System

5.2.2.1 Aim of the Model

This case study is designed to estimate the impact of all individual roots to the overall root system dynamics. We use the model of Leitner et al. (2010a) to study (1) the effect of root system architecture and branching structure on overall root system P_i uptake and soil P_i depletion, and (2) root system development as affected by P_i concentrations in soil. The latter includes feedback between soil P_i concentration and root system development, including chemotropism.

5.2.2.2 Model Description

The focus here is on P_i uptake, neglecting water movement. We consider a maize root system growing in a conical pot (height 10 cm, top diameter 10 cm, bottom diameter 6 cm). The simulation starts with five germinating seeds at the top of the pot. The P_i concentration of the left half of the pot differs from that on the right half, and our aim is to quantify the effect of this difference on root system development and P_i uptake.

We simulate the development of root system architecture with the three-dimensional L-system model of Leitner et al. (2010a). The Matlab code is freely available online (Schnepf and Klepsch 2010). This model is similar to other root architecture models such as RootMap (Claassen et al. 2006; Diggle 1988) or RootTyp (Pages et al. 2004) in that root growth parameters are predetermined for each topological order. All parameter values are given by mean value and standard deviation [see Leitner et al. (2010a) for a full table of model parameters]. The model also provides a simple way to include different kinds of tropisms such as gravitropism, chemotropism and thigmotropism. The latter can be used to define a geometry, e.g. a pot, within which root growth is confined. All tropisms are implemented by a random optimisation algorithm, which is independent of the spatial discretisation along the root axis. The outcome of the root growth model is a root system composed of individual root segments. The information stored for each segment includes length, radius, position and age.

We describe P_i diffusion in soil and nutrient uptake by the root system with (5.10)–(5.12) (Barber 1995; Tinker and Nye 2000):

$$(\theta + b)\frac{\partial c}{\partial t} = \nabla \cdot (D\theta f \nabla c) - F\,, \tag{5.10}$$

$$c = c_0 \quad \text{at} \qquad t = 0\,, \tag{5.11}$$

$$(D\theta f \nabla c) \cdot \mathbf{n} = 0 \quad \text{at} \qquad \mathbf{x} \in \partial\Omega, \tag{5.12}$$

where c is phosphate concentration in soil solution, t time, $\mathbf{x}$ space vector, θ volumetric water content, b buffer power, f impedance factor, D diffusion coefficient in water, c_0 initial P_i concentration in soil solution, F volumetric sink term for root P_i uptake, $\partial\Omega$ domain boundary, and $\mathbf{n}$ outer normal vector. The domain Ω is a conical pot with a height of 10 cm, a top diameter of 10 cm and a bottom diameter of 6 cm (see Fig. 5.5). Boundary condition (5.12) ensures that P_i cannot diffuse out of the domain.

The diffusion equation, (5.10), is coupled with the root system growth model via the sink term F, which represents the average root uptake in a representative elementary volume (REV). We determine F by summing over the P_i uptake of every root segment within each REV,

$$F = \frac{1}{\text{REV}} \sum_{s=1}^{N} 2 a_s \pi l_s F_s, \tag{5.13}$$

where a_s is radius of root segment, F_s influx into a root segment, l_s root segment length, N number of root segments within REV. Water and solute transport models with sink terms for root uptake generally neglect depletion zones around individual roots (Claassen et al. 2006). In order to calculate the flux into a root segment, we account for the dynamic development of a P_i depletion zone according to the approximate analytical solution of Roose et al. (2001) given by (5.14):

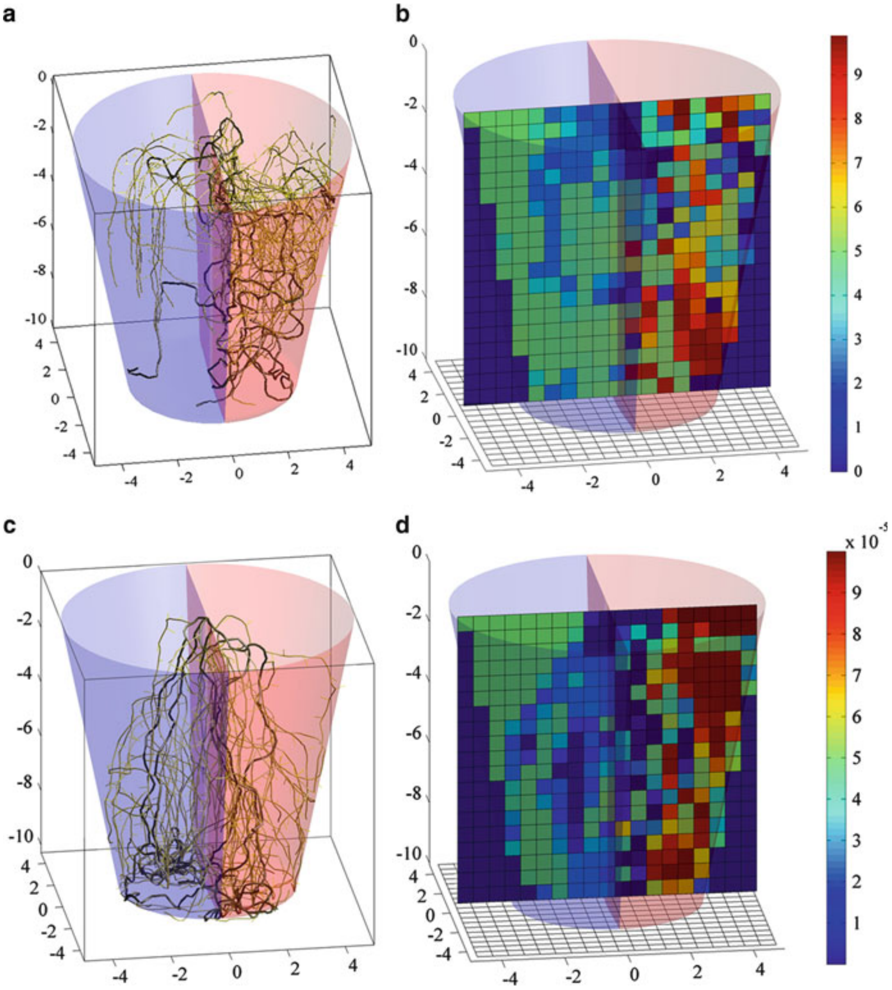

Fig. 5.5 Root system development and soil P_i depletion after 20 days. Initial P_i concentration in pot 1×10^{-4} µmol cm^{-3} (*right half*) and 0.5×10^{-4} µmol cm^{-3} (*left half*). (**a**) Root system growth according to chemotropism. (**b**) Soil depletion due to root system shown in (**a**). (**c**) Root system growth according to gravitropism only. (**d**) Soil depletion due to root system shown in (**c**)

$$
\begin{aligned}
F_{\mathrm{s}}(t_{\mathrm{s}}, a_{\mathrm{s}}) &= \frac{2F_m c_\infty}{1 + c_\infty + L(t_s) + \sqrt{4c_\infty + [1 - c_\infty + L(t_{\mathrm{s}})]^2}}, \\
c_\infty &= c_0/K_m, \\
L(t_s, a_s) &= \frac{F_m a_s}{2\theta D f K_m} \ln\left(4\mathrm{e}^{-\gamma} \frac{\theta D f}{(\theta + b) a_s{}^2} t_s + 1\right),
\end{aligned}
\tag{5.14}
$$

where $\gamma = 0.5772$ is Euler's constant, t_s age of root segment, F_m maximal P_i influx into root and K_m Michaelis–Menten constant. Equations (5.13) and (5.14) yield a volumetric sink term F that depends on (1) the age of each root segment, (2) the number of root segments in the REV and (3) the size of the REV.

The cubic REVs act as spatial discretisation used for the numerical solution of (5.10)–(5.12). For every REV a sink term is created according to (5.13). The REV must be large enough to regard the roots in a single REV as root densities, but small enough to represent root density variations of the root system. Here, we choose an REV size of 0.5^3 cm^3. For the numerical solution, we use the Crank–Nicholson finite difference scheme. The nonlinear sink term is solved by using fixed-point iteration. The time step Δt is chosen such that the Courant–Friedrichs–Lewy (CFL) condition for the diffusive case, $\Delta t \leq \Delta x^2/2D$, is fulfilled. Note that the CFL condition is a necessary condition for the convergence of numerical solutions of partial differential equations (Morton and Mayers 1994).

In this case study, we examine the effect of inhomogeneous initial P_i distribution on root system development, soil P_i depletion and P_i uptake. Root growth parameters for a maize root system are taken from Leitner et al. (2010a), and the soil parameters and P_i uptake parameters for maize from Roose et al. (2001). We consider a pot in which the initial concentration in the left half is half that in the right. This is illustrated by the blue and red colour in Fig. 5.5. At the top of the pot, five seeds are initially present and grow according to the model of Leitner et al. (2010a). All simulations assume that gravitropism, i.e. the tendency of the root to grow downwards, occurs. We also study the effect when the root system does or does not additionally follow chemotropism, i.e. the tendency of the roots to grow towards higher P_i concentrations.

5.2.2.3 Results

Figure 5.5a, b shows the root system and soil P_i depletion after 20 days, when roots tend to grow towards higher P_i concentrations (chemotropism). Figure 5.5c, d shows the same when the root system only follows gravitropism but not chemotropism. In this example, overall root length is the same in both cases and only the positions of the roots differ. In the case of chemotropism, the root system is denser in the right part of the pot, where the initial P_i concentration was higher. Therefore, depletion is less in the left part of the pot. In the case of no chemotropism, root length densities are similar in both halves, equally depleting both parts of the pot.

Chemotropism enhanced P_i depletion in the region with higher P_i concentration and thus increased overall P_i uptake by that root system as compared to the root system without chemotropism (see Fig. 5.6).

5.2.2.4 Discussion and Outlook

This case study uses a model that considers two spatial scales: the root system scale and the single root scale. Uptake and depletion caused by individual roots is described on the single root scale, whereas overall P_i transport and uptake is described on root system scale. The sink term is created by averaging over a REV.

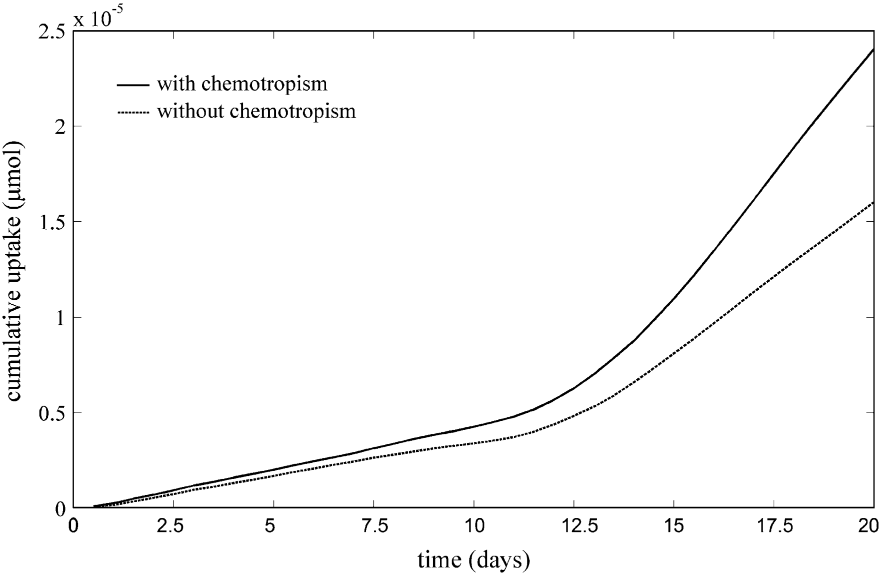

Fig. 5.6 Cumulative P_i uptake by root systems, with and without chemotropism

We consider dynamic development of the depletion zone around each root, but neglect inter-root competition. This is valid for sparingly soluble nutrients such as P_i.

This example quantifies the effect of chemotropism on P_i uptake. The overall root length of the root systems was the same in the two cases considered (chemotropism and no chemotropism). However, root surface area was 4.6 times denser in the high concentration region in the case of chemotropism, whereas it was approximately equal in both pot halves in the case of gravitropism only. Thus, chemotropism yielded a 1.5-fold increase of P_i uptake.

In addition to the plastic responses of the root system to nutrient-rich patches, growth and uptake rates can be affected (Claassen et al. 2006). Further challenges for future model development include coupling the model to a model of soil water movement, upscaling of additional single root traits (e.g. root exudation and mycorrhizas) to the root system scale, and the explicit modelling of organic P dynamics.

5.2.3 P Uptake and Crop Response to Soil P Levels

5.2.3.1 Aim of the Model

Most nutrient models combine the equation describing the radial movement of ions from soil to root surface by diffusion and mass flow with an equation relating root uptake to the ion concentration at the root surface. In the former, the interactions of the ion with the soil solid phase are also considered. An integration procedure allows the calculation of nutrient uptake by the whole root system (Barber 1995; Tinker and Nye 2000). Such models were successfully evaluated on short periods and were useful tools for investigation of the mechanisms at the rhizosphere scale. Nevertheless, these classical models often failed to predict nutrient uptake over long periods because the feedback effects between nutrient uptake and plant functions were poorly accounted for.

The aim of this case study is to illustrate how to include crop growth response in nutrient uptake models and the ability of such models to provide a basis for assessing target values for soil nutrient concentration. In order to do so, we developed a mechanistic model that combined an ecophysiological model and a root nutrient uptake model (Mollier et al. 2008). A mechanistic model for the simultaneous simulation of P_i supply, its uptake by the root system and the crop growth response is presented. The dynamic link between these processes was explicitly taken into account. This model was used to simulate P_i uptake and maize crop response in field conditions under three levels of soil P_i availability (high P, intermediate P and low P). All parameters and input variables are given in Mollier et al. (2008). Secondly, we simulated P_i uptake and crop growth for a wide range of soil P_i concentration to determine target values for soil P_i availability.

5.2.3.2 Model Description

The proposed model consists of three modules that are closely connected (Fig. 5.7). The first module deals with crop growth based on crop phenology and biomass accumulation depending on climatic conditions, and on crop P demand derived from potential crop growth depending on the environmental conditions. The second module describes P_i supply from the soil, considering the ion P_i concentration in soil solution and the soil buffer capacity. The third module deals with crop P_i uptake depending on crop P demand and P_i uptake capacity determined by the soil P_i supply and root length density distribution in the soil profile. The three modules are integrated to simulate the feedback loop of effective P_i uptake on crop growth. The actual shoot and root growth are adjusted according P_i uptake. Thus, the model tightly couples crop growth with soil processes.

Module 1: Modelling Crop Growth and Crop P Demand

The crop growth module simulates crop phenology and dry matter accumulation as a function of daily temperature and the photosynthetically active radiation absorbed by the canopy (PAR_a) and its conversion into dry biomass (Monteith 1977). The daily biomass produced is partitioned between shoot and root, assuming that shoot demand for carbohydrates is satisfied first. The remaining carbohydrates are allocated to the root system. The daily crop P demand is derived from the potential leaf expansion rate allowed by temperature and the carbohydrate availability using a

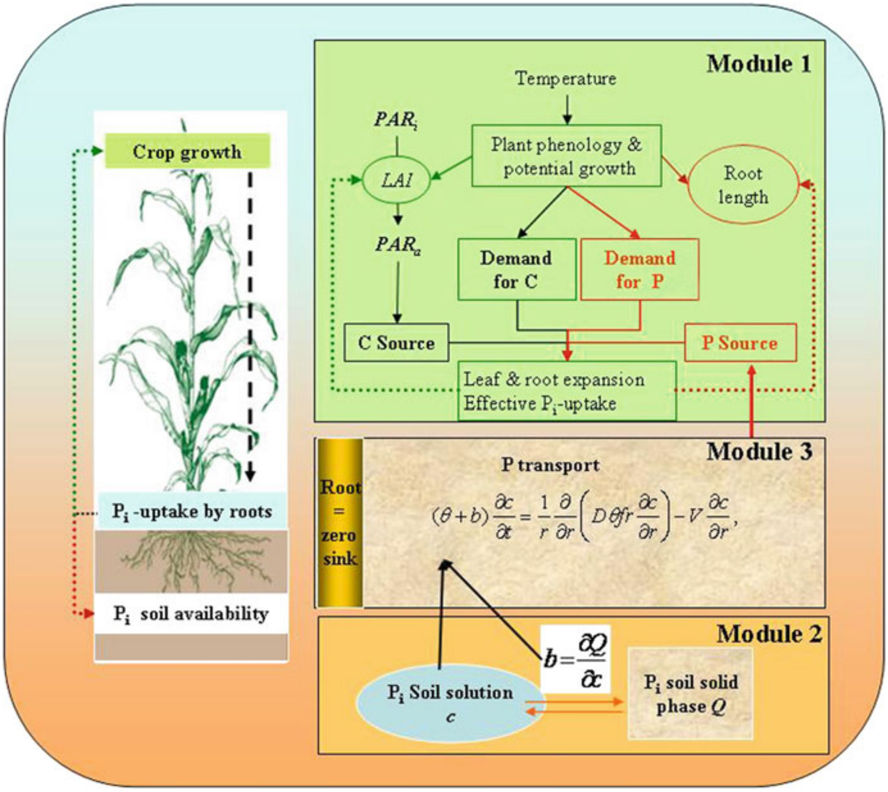

Fig. 5.7 Schematic representation of P_i uptake model including crop P response (adapted from Mollier et al. 2008)

close relationship between leaf area index (LAI) and total crop P_i uptake obtained under non-limiting conditions.

Module 2: Modelling Soil P Supply to Crops

Phosphate soil availability refers to the concentration of P_i in soil solution (c mg mL^{-1}) plus the amount of P_i (Q mg cm^{-3}) associated to the solid phase, which is in equilibrium with soil solution P_i. The relationship between c and Q is described by a Freundlich equation (McGechan and Lewis 2002):

$$Q = k_f c^n. \tag{5.15}$$

The soil buffer capacity is the ratio of changes in solid P_i to those in solution:

$$b = \frac{\partial Q}{\partial c}, \tag{5.16}$$

where k_f and n are Freundlich coefficients determined from a sorption/desorption experiment and b is the soil buffer capacity.

Module 3: Modelling P Uptake by the Root System According to Crop P Demand and Soil P Supply

The two-dimensional soil domain is subdivided into square control volumes (5×5 cm). Each of these is characterised by soil properties and root length density. The equations for P_i transport by mass flow and diffusion within the solution of the soil cylinder around the root and P_i uptake are used for each control volume:

$$(\theta + b)\frac{\partial c}{\partial t} = \frac{1}{r}\frac{\partial}{\partial r}\left(D\theta fr\frac{\partial c}{\partial r}\right) - V\frac{\partial c}{\partial r}, \tag{5.17}$$

$$c = c_0 \quad \text{at} \quad t = 0\,. \tag{5.18}$$

The boundary condition at the root surface follows from crop P demand (S_{sr} mg cm^{-2} day^{-1}):

$$-D\theta f\frac{\partial c}{\partial r} + Vc = -\frac{S_{sr}}{2\pi r_0 \Delta z L_{rv}} \quad \text{at} \quad r = r_0, \tag{5.19}$$

$$-D\theta f\frac{\partial c}{\partial r} + Vc = 0 \quad \text{at} \quad r = r_1, \tag{5.20}$$

where c is phosphate concentration in soil solution, t time, r radial distance from root axis, θ volumetric water content, b buffer power, f impedance factor, D diffusion coefficient in water, V flux of water toward root, c_0 initial P_i concentration in soil solution, r_0 root radius, $r_1 = 1/\sqrt{\pi L_{rv}}$ mean half distance between roots calculated for each control volume, L_{rv} root length density and Δz thickness of control volume.

Required uptake cannot occur when the diffusion and mass flow processes in soil cannot replenish enough P_i to the root. We assume that the maximum uptake rate equals the maximum possible rate of transport (by diffusion and mass flow) to the root, i.e. the root behaves as a zero sink. The maximum nutrient uptake rate per unit surface area S_{sm} (mg cm^{-2} day^{-1}) is derived from the steady-rate approximate solution for the concentration profile around the root for the zero sink condition (De Willigen and Van Noordwijk 1994):

$$S_{\text{sm}} = 2\pi \Delta z L_{\text{rv}} D \frac{(\rho^2 - 1)}{2G(\rho, v)}\overline{P}\,, \tag{5.21}$$

where $\overline{P}$ is the average P_i in soil surrounding the root, ρ the dimensionless radius and $G(\rho,v)$ is a geometry function (see Mollier et al. 2008).

Actual P_i uptake may or may not satisfy crop P demand. We assume that the actual P_i uptake rate S_s equals the required P_i uptake rate S_{sr} as long as S_{sr} is less than the maximum P_i uptake rate S_{sm}, otherwise S_{sr} equals the maximum P_i uptake rate S_{sm}. The total P_i uptake by the entire root system is the sum of P_i uptake from all control volumes.

Integration and Feedback Loop

Shoot and root growth are calculated from carbohydrate assimilation and the actual P_i uptake. If crop P demand is satisfied, effective crop growth is only limited by carbohydrate assimilation and climatic conditions. If actual P_i uptake is less than required, leaf area expansion is reduced, so that more carbohydrates are allocated to the root system. The new root distribution in the soil is derived from the biomass allocated to the root and is distributed in the soil based on the diffusion-type root growth model proposed by (De Willigen et al. 2002). The nutrient transport equation is explicitly solved with a time step that is restricted according to the ratio of the Courant and Peclet numbers (Daus et al. 1985).

5.2.3.3 Results

Figure 5.8a shows predicted cumulated P_i uptake as function of soil P_i levels. In this example, P_i uptake was reduced as soil P_i level decreased. This reduction was more pronounced for low-P treatment. The simulated crop growth response to P_i uptake is shown in Fig. 5.8b, c. For high-P treatment, leaf area expansion and root growth were only governed by climatic conditions and biomass partitioning within the plant. For intermediate-P treatment, leaf area expansion was slightly reduced, whereas root growth was almost not affected. For low-P treatment, both shoot and root growths were reduced in response to low P_i uptake. Moreover, limitation

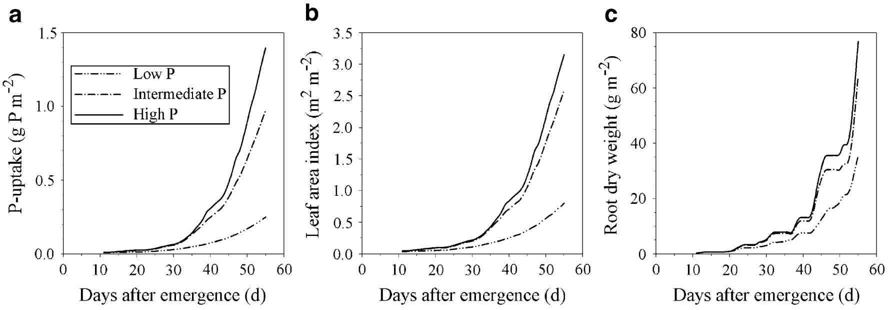

Fig. 5.8 Simulation of (**a**) cumulative P_i uptake by crop (g P_i m^{-2}), (**b**) leaf area index (m^2 m^{-2}) and (**c**) root biomass (g m^{-2}) versus time elapsed since emergence, for three P_i soil levels (low, intermediate and high P)

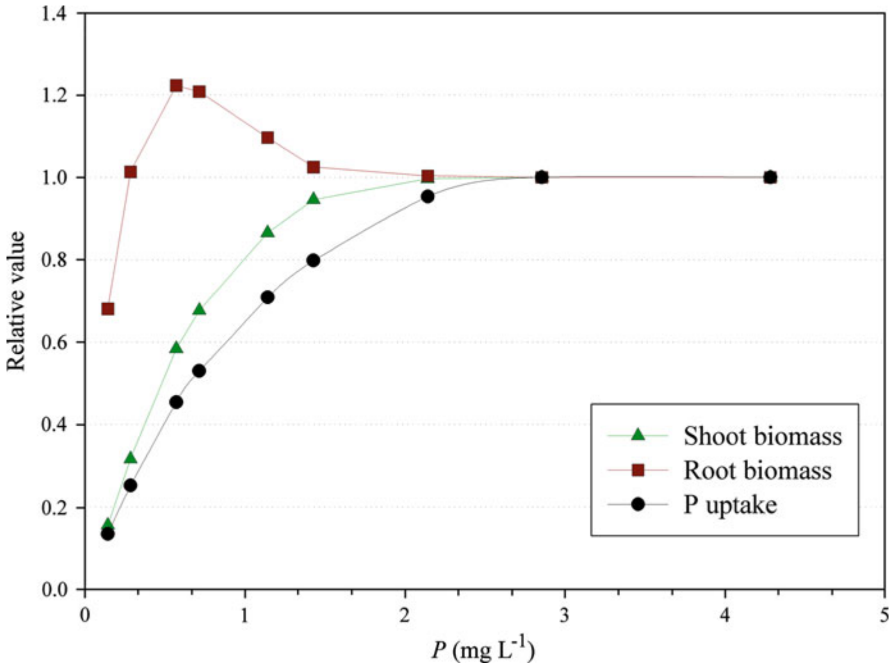

Fig. 5.9 Relative values of P_i uptake, shoot and root biomass (simulated value until 60 days after emergence divided by simulated value under high P_i conditions) as a function of P_i soil solution concentration (in mg P L^{-1}) for a sandy soil

in soil P_i supply reduced first leaf area, and assimilates no longer needed for leaf expansion rate were allocated to the root. Consequently, under low-P treatment the root growth was less affected than shoot growth and root-to-shoot ratio was increased.

In Fig. 5.9, the relative P_i uptake, shoot dry biomass and root biomass predicted by the proposed model were plotted versus the concentration of P_i in the soil solution. As P_i decreased under a threshold value, both P_i uptake and shoot growth were reduced, whereas relative root growth was maintained or increased. Such crop response allowed the root system to increase the soil volume explored and consequently the access to soil P_i. However, for very low P_i supply, such crop response could not fully counter the P_i shortage. The threshold value for P_i is dependent on crops, soil P_i supply properties (mainly b, θ and f) and climatic conditions.

5.2.3.4 Discussion and Outlook

The presented model is a mechanistic model that explicitly includes a feedback loop between nutrient uptake and crop growth. The simulated crop responses are consistent with those commonly reported when P_i is limiting. Increases in root-to-shoot ratio were observed under P_i shortage (Lynch 2007). Moreover, the causes of these increases are consistent with experimental results of Wissuwa et al. (2005) and Mollier and Pellerin (1999). Limitation in soil P_i supply reduces first leaf area, and assimilates no longer needed for leaf expansion rate are partitioned to the roots. Once these excess assimilates are used up, the smaller leaf area no longer supplies enough carbohydrates and, consequently, root growth decreases due to carbohydrate limitation.

This case study illustrates the possible use of a nutrient uptake model including crop growth response to explore a wide range of situations. Such a model explicitly accounts for the numerous soil and crop factors that interact with nutrient supply and uptake. Although progress is still needed (including uptake by mycorrhizal roots, root tropism, rhizosphere processes etc.) such a model can provide a basis for both improving scientific knowledge on soil–crop transfer of minerals and assessing target values for soil nutrient availability in a specific context.

5.3 Summary

Mathematical modelling is important in enhancing our understanding of the complex processes in plant phosphate nutrition, particularly where processes are difficult to assess experimentally. This chapter illustrates the model-building process for plant phosphate uptake models, focusing on different plant traits that enhance phosphate uptake.

All models presented in this chapter are mechanistically based as well as deterministic, and are based on partial differential equations. Mechanistic mathematical models help to enhance our understanding of phenomena occurring across different spatial and temporal scales (Roose and Schnepf 2008). Close collaboration between experimentalists and modellers is necessary for model validation and parameterisation and will further enhance scientific progress. In this respect, modelling could assist in crop management and breeding of crops with traits that are beneficial, for example in low nutrient environments.

References

Arheimer B, Andersson L, Larsson M, Lindström G, Olsson J, Pers BC (2004) Modelling diffuse nutrient flow in eutrophication control scenarios. Water Sci Technol 49:37–45

Barber SA (1995) Soil nutrient bioavailability: a mechanistic approach. Wiley, New York

Bhadoria PS, Steingrobe B, Claassen N, Liebersbach H (2002) Phosphorus efficiency of wheat and sugar beet seedlings grown in soils with mainly calcium, or iron and aluminium phosphate. Plant Soil 246:41–52

Bucher M (2007) Functional biology of plant phosphate uptake at root and mycorrhiza interfaces. New Phytol 173:11–26

Chung SO, Kim HS, Kim JS (2003) Model development for nutrient loading from paddy rice fields. Agric Water Manage 62:1–17

Claassen N, De Willigen P, Diederik J, Doussan C, Dunbabin V, Heinen M, Hopmans JW, Kirk G, Kuzyakov Y, Mayer U, Mollier A, Nietfeld H, Nowack B, Oswald S, Roose T, Schnepf A, Schulin R, Seuntjens P, Silk WK, Steingrobe B, van Beinum W, Van Bodegom P (2006) Rhizosphere models. In: Luster J et al (eds) Handbook of methods used in rhizosphere research, part II. Swiss Federal Research Institute WSL, Birmensdorf, pp 487–517

Dalzell BJ, Gowda PH, Mulla DJ (2004) Modeling sediment and phosphorus losses in an agricultural watershed to meet TMDLs. J Am Water Resour Assoc 40:533–543

Darrah PR, Jones DL, Kirk GJD, Roose T (2006) Modelling the rhizosphere: a review of methods for 'upscaling' to the whole-plant scale. Eur J Soil Sci 57:13–25

Daus AD, Frind EO, Sudicky EA (1985) Comparative error analysis in finite-element formulations of the advection-dispersion equation. Adv Water Resour 8:86–95

De Willigen P, Van Noordwijk M (1994) Mass flow and diffusion of nutrients to a root with constant or zero-sink uptake. II. Zero-sink uptake. Soil Sci 157:171–175

De Willigen P, Heinen M, Mollier A, Van Noordwijk M (2002) Two-dimensional growth of a root system modelled as a diffusion process. I. Analytical solutions. Plant Soil 240:225–234

Diggle AJ (1988) Rootmap – a model in three-dimensional coordinates of the growth and structure of fibrous root systems. Plant Soil 105:169–178

Djodjic F, Montas H, Shirmohammadi A, Bergström L, Ulén B (2002) A decision support system for phosphorus management at a watershed scale. J Environ Qual 31:937–945

Dunbabin VM, Armstrong RD, Officer SJ, Norton RM (2009) Identifying fertiliser management strategies to maximise nitrogen and phosphorus acquisition by wheat in two contrasting soils from Victoria, Australia. Aust J Soil Res 47:74–90

Einstein A (1934) On the method of theoretical physics. Philos Sci 1:163–169

Fitter AH, Gilligan CA, Hollingworth K, Kleczkowski A, Twyman RM, Pitchford JW (2005) Biodiversity and ecosystem function in soil. Funct Ecol 19:369–377

Frossard E, Condron LM, Oberson A, Sinaj S, Fardeau JC (2000) Processes governing phosphorus availability in temperate soils. J Environ Qual 29:15–23

Ge ZY, Rubio G, Lynch JP (2000) The importance of root gravitropism for inter-root competition and phosphorus acquisition efficiency: results from a geometric simulation model. Plant Soil 218:159–171

Giasson E, Bryant RB, Bills NL (2002) Environmental and economic optimization of dairy manure management: a mathematical programming approach. Agron J 94:757–766

Gillespie AR, Pope PE (1990) Rhizosphere acidification increases phosphorus recovery of black locust. II. Model predictions and measured recovery. Soil Sci Soc Am J 54:538–541

Grant RF, Robertson JA (1997) Phosphorus uptake by root systems: mathematical modelling in ecosys. Plant Soil 188:279–297

Grant RF, Amrani M, Heaney DJ, Wright R, Zhang M (2004) Mathematical modeling of phosphorus losses from land application of hog and cattle manure. J Environ Qual 33:210–231

Harrison JA, Seitzinger SP, Bouwman AF, Caraco NF, Beusen AHW, Vörösmarty CJ (2005) Dissolved inorganic phosphorus export to the coastal zone: results from a spatially explicit, global model. Global Biogeochem Cycles 19:1–15

Hoffmann C, Ladewig E, Claassen N, Jungk A (1994) Phosphorus uptake of maize as affected by ammonium and nitrate nitrogen – Measurements and model calculations. Journal of Plant Nutrition and Soil Science 157:225–232

Huguenin-Elie O, Kirk GJD, Frossard E (2009) The effects of water regime on phosphorus responses of rainfed lowland rice cultivars. Ann Bot 103:211–220

Jakobsen I, Abbott LK, Robson AD (1992) External hyphae of vesicular-arbuscular mycorrhizal fungi associated with *Trifolium subterraneum L.* 1. Spread of hyphae and phosphorus inflow into roots. New Phytol 120:371–380

Janssen PHM, Heuberger PSC (1995) Calibration of process-oriented models. Ecol Modell 83:55–66

Kirk GJD (1999) A model of phosphate solubilization by organic anion excretion from plant roots. Eur J Soil Sci 50:369–378

Kirschbaum MUF, Medlyn BE, King DA, Pongracic S, Murty D, Keith H, Khanna PK, Snowdon P, Raison RJ (1998) Modelling forest-growth response to increasing CO_2 concentration in relation to various factors affecting nutrient supply. Glob Change Biol 4:23–41

Lambers H, Shane MW, Cramer MD, Pearse SJ, Veneklaas EJ (2006) Root structure and functioning for efficient acquisition of phosphorus: matching morphological and physiological traits. Ann Bot 98:693–713

Landis FC, Fraser LH (2008) A new model of carbon and phosphorus transfers in arbuscular mycorrhizas. New Phytol 177:466–479

Leitner D, Klepsch S, Bodner G, Schnepf A (2010a) A dynamic root system growth model based on L-systems. Tropisms and coupling to nutrient uptake from soil. Plant Soil 332:177–192

Leitner D, Klepsch S, Ptashnyk M, Marchant A, Kirk GJD, Schnepf A, Roose T (2010b) A dynamic model of nutrient uptake by root hairs. New Phytol 185:792–802

Li X-L, George E, Marschner H (1991) Extension of the phosphorus depletion zone in VA-mycorrhizal white clover in a calcareous soil. Plant Soil 136:41–48

Luster J, Göttlein A, Nowack B, Sarret G (2009) Sampling, defining, characterising and modeling the rhizosphere – the soil science tool box. Plant Soil 321:457–482

Lynch JP (2007) Roots of the second green revolution. Aust J Bot 55:493–512

McGechan MB, Lewis DR (2002) Sorption of phosphorus by soil, part 1: principles, equations and models. Biosystems Eng 82:1–24

Migliaccio KW, Chaubey I, Haggard BE (2007) Evaluation of landscape and instream modeling to predict watershed nutrient yields. Environ Modell Softw 22:987–999

Mollier A, Pellerin S (1999) Maize root system growth and development as influenced by phosphorus deficiency. J Exp Bot 50:487–497

Mollier A, De Willigen P, Heinen M, Morel C, Schneider A, Pellerin S (2008) A two-dimensional simulation model of phosphorus uptake including crop growth and P-response. Ecol Modell 210:453–464

Monteith JL (1977) Climate and the efficiency of crop production in Britain. Philos Trans R Soc London B 281:277–294

Morton KW, Mayers DF (1994) Numerical solution of partial differential equations. Cambridge University Press, Cambridge

Overman AR, Scholtz RV (1999) Langmuir-Hinshelwood model of soil phosphorus kinetics. Commun Soil Sci Plant Anal 30:109–119

Pages L, Vercambre G, Drouet JL, Lecompte F, Collet C, Le Bot J (2004) RootTyp: a generic model to depict and analyse the root system architecture. Plant Soil 258:103–119

Porder S, Vitousek PM, Chadwick OA, Chamberlain CP, Hilley GE (2007) Uplift, erosion, and phosphorus limitation in terrestrial ecosystems. Ecosystems 10:158–170

Ptashnyk M, Roose T, Kirk GJD (2010) Diffusion of strongly sorbed solutes in soil: a dual-porosity model allowing for slow access to sorption sites and time-dependent sorption reactions. Eur J Soil Sci 61:108–119

Radcliffe DE, Lin Z, Risse LM, Romeis JJ, Jackson CR (2009) Modeling phosphorus in the Lake Allatoona watershed using SWAT. I. Developing phosphorus parameter values. J Environ Qual 38:111–120

Raghothama KG, Karthikeyan AS (2005) Phosphate acquisition. Plant Soil 274:37–49

Reginato JC, Palumbo MC, Moreno IS, Bernardo IC, Tarzia DA (2000) Modeling nutrient uptake using a moving boundary approach: comparison with the Barber-Cushman model. Soil Sci Soc Am J 64:1363–1367

Roose T, Fowler AC (2004) A mathematical model for water and nutrient uptake by plant root systems. J Theor Biol 228:173–184

Roose T, Schnepf A (2008) Mathematical models of plant-soil interaction. Philos Trans R Soc London A 366:4597–4611

Roose T, Fowler AC, Darrah PR (2001) A mathematical model of plant nutrient uptake. J Math Biol 42:347–360

Saltelli A, Chan K, Scott EM (eds) (2000) Sensitivity analysis. Wiley series on probability and statistics. Wiley, Chichester

Schils RLM, De Haan MHA, Hemmer JGA, Van Den Pol-van DA, De Boer JA, Evers AG, Holshof G, Van Middelkoop JC, Zom RLG (2007) DairyWise, a whole-farm dairy model. J Dairy Sci 90:5334–5346

Schlecht E, Hiernaux P (2005) Beyond adding up inputs and outputs: process assessment and upscaling in modelling nutrient flows. Nutr Cycl Agroecosyst 70:303–319

Schnepf A, Klepsch S (2010) Mathematics and rhizotechnology. Mathematical methods for upscaling of rhizosphere control mechanisms. BOKU – University of Natural Resources and Applied Life Sciences, Vienna. http://www.boku.ac.at/marhizo/. Accessed 23 July 2010

Schnepf A, Roose T (2006) Modelling the contribution of arbuscular mycorrhizal fungi to plant phosphate uptake. New Phytol 171:669–682

Schnepf A, Roose T, Schweiger P (2008a) Growth model for arbuscular mycorrhizal fungi. J R Soc Interface 5:773–784

Schnepf A, Roose T, Schweiger P (2008b) Impact of growth and uptake patterns of arbuscular mycorrhizal fungi on plant phosphorus uptake – a modelling study. Plant Soil 312:85–99

Schoumans OF, Groenendijk P (2000) Modeling soil phosphorus levels and phosphorus leaching from agricultural land in the Netherlands. J Environ Qual 29:111–116

Shi Z, Erickson LE (2001) Mathematical model development and simulation of in situ stabilization in lead-contaminated soils. J Hazard Mater 87:99–116

Smethurst PJ, Comerford NB (1993) Potassium and phosphorus uptake by competing pine and grass: observations and model verification. Soil Sci Soc Am J 57:1602–1610

Smith J, Smith P (2007) Introduction to environmental modelling. Oxford University Press, New York

Smith SE, Smith FA, Jakobsen I (2003) Mycorrhizal fungi can dominate phosphate supply to plants irrespective of growth responses. Plant Physiol 130:16–20

Teklić T, Vukadinović V, Lončarić Z, Rengel Z, Dropulić D (2002) Model for optimizing fertilization of sugar beet, wheat, and maize grown on pseudogley soils. J Plant Nutr 25:1863–1879

Tinker PB, Nye PH (2000) Solute movement in the rhizosphere. Oxford University Press, New York

Torbert HA, Gerik TJ, Harman WL, Williams JR, Magre M (2008) EPIC evaluation of the impact of poultry litter application timing on nutrient losses. Commun Soil Sci Plant Anal 39:3002–3031

Van Der Zee SEATM, Van Riemsdijk WH (1991) Model for the reaction kinetics of phosphate with oxides and soil. In: Bolt GH et al (eds) Interactions at the soil colloid–soil solution interface. Kluwer Academic, Dordrecht, pp 205–239

Wang YP, Houlton BZ, Field CB (2007) A model of biogeochemical cycles of carbon, nitrogen, and phosphorus including symbiotic nitrogen fixation and phosphatase production. Global Biogeochem Cycles 21:1–15

Wissuwa M, Gamat G, Ismail AM (2005) Is root growth under phosphorus deficiency affected by source or sink limitations? J Exp Bot 56:1943–1950